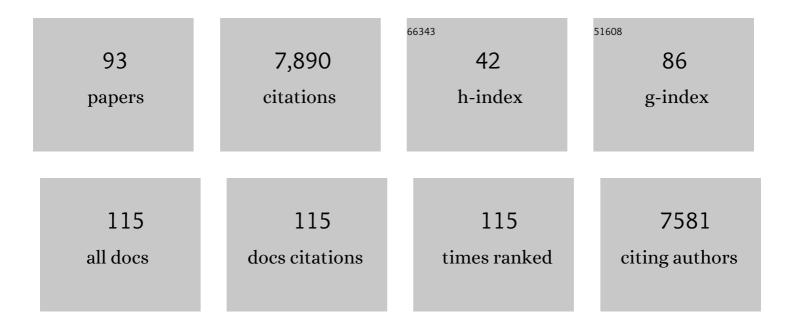
Isabel Trigo

List of Publications by Year in descending order

Source: https://exaly.com/author-pdf/1744576/publications.pdf Version: 2024-02-01



ISAREL TRICO

#	Article	IF	CITATIONS
1	Satellite-derived land surface temperature: Current status and perspectives. Remote Sensing of Environment, 2013, 131, 14-37.	11.0	1,545
2	IMILAST: A Community Effort to Intercompare Extratropical Cyclone Detection and Tracking Algorithms. Bulletin of the American Meteorological Society, 2013, 94, 529-547.	3.3	391
3	Objective Climatology of Cyclones in the Mediterranean Region. Journal of Climate, 1999, 12, 1685-1696.	3.2	383
4	Climatology of Cyclogenesis Mechanisms in the Mediterranean. Monthly Weather Review, 2002, 130, 549-569.	1.4	275
5	Google Earth Engine Open-Source Code for Land Surface Temperature Estimation from the Landsat Series. Remote Sensing, 2020, 12, 1471.	4.0	263
6	Climatology and interannual variability of storm-tracks in the Euro-Atlantic sector: a comparison between ERA-40 and NCEP/NCAR reanalyses. Climate Dynamics, 2006, 26, 127-143.	3.8	244
7	An assessment of remotely sensed land surface temperature. Journal of Geophysical Research, 2008, 113, .	3.3	210
8	The Outstanding 2004/05 Drought in the Iberian Peninsula: Associated Atmospheric Circulation. Journal of Hydrometeorology, 2007, 8, 483-498.	1.9	208
9	The Satellite Application Facility for Land Surface Analysis. International Journal of Remote Sensing, 2011, 32, 2725-2744.	2.9	207
10	How exceptional was the early August 2003 heatwave in France?. Geophysical Research Letters, 2005, 32, .	4.0	203
11	Shallow and deep landslides induced by rainfall in the Lisbon region (Portugal): assessment of relationships with the North Atlantic Oscillation. Natural Hazards and Earth System Sciences, 2005, 5, 331-344.	3.6	190
12	Climate impact of the European winter blocking episodes from the NCEP/NCAR Reanalyses. Climate Dynamics, 2004, 23, 17-28.	3.8	187
13	Understanding Precipitation Changes in Iberia in Early Spring: Weather Typing and Storm-Tracking Approaches. Journal of Hydrometeorology, 2006, 7, 101-113.	1.9	184
14	Quantifying the Uncertainty of Land Surface Temperature Retrievals From SEVIRI/Meteosat. IEEE Transactions on Geoscience and Remote Sensing, 2010, 48, 523-534.	6.3	142
15	Decline in Mediterranean rainfall caused by weakening of Mediterranean cyclones. Geophysical Research Letters, 2000, 27, 2913-2916.	4.0	124
16	A climatological assessment of drought impact on vegetation health index. Agricultural and Forest Meteorology, 2018, 259, 286-295.	4.8	118
17	Validation of remotely sensed surface temperature over an oak woodland landscape — The problem of viewing and illumination geometries. Remote Sensing of Environment, 2014, 148, 16-27.	11.0	105
18	Long Term Validation of Land Surface Temperature Retrieved from MSG/SEVIRI with Continuous in-Situ Measurements in Africa. Remote Sensing, 2016, 8, 410.	4.0	100

#	Article	IF	CITATIONS
19	Chapter 6 Cyclones in the Mediterranean region: Climatology and effects on the environment. Developments in Earth and Environmental Sciences, 2006, 4, 325-372.	0.1	99
20	The Impact of North Atlantic Wind and Cyclone Trends on European Precipitation and Significant Wave Height in the Atlantic. Annals of the New York Academy of Sciences, 2008, 1146, 212-234.	3.8	99
21	Thermal Land Surface Emissivity Retrieved From SEVIRI/Meteosat. IEEE Transactions on Geoscience and Remote Sensing, 2008, 46, 307-315.	6.3	99
22	Satellite and In Situ Observations for Advancing Global Earth Surface Modelling: A Review. Remote Sensing, 2018, 10, 2038.	4.0	95
23	A review of earth surface thermal radiation directionality observing and modeling: Historical development, current status and perspectives. Remote Sensing of Environment, 2019, 232, 111304.	11.0	91
24	Land surface temperature from multiple geostationary satellites. International Journal of Remote Sensing, 2013, 34, 3051-3068.	2.9	85
25	Klaus – an exceptional winter storm over northern Iberia and southern France. Weather, 2011, 66, 330-334.	0.7	83
26	Objective climatology of cyclones in the Mediterranean region: a consensus view among methods with different system identification and tracking criteria. Tellus, Series A: Dynamic Meteorology and Oceanography, 2022, 68, 29391.	1.7	79
27	Are Greenhouse Gas Signals of Northern Hemisphere winter extra-tropical cyclone activity dependent on the identification and tracking algorithm?. Meteorologische Zeitschrift, 2013, 22, 61-68.	1.0	77
28	The state of climate in NW Iberia. Climate Research, 2011, 48, 109-144.	1.1	77
29	Meteosat Land Surface Temperature Climate Data Record: Achievable Accuracy and Potential Uncertainties. Remote Sensing, 2015, 7, 13139-13156.	4.0	74
30	The Influence of the North Atlantic Oscillation on Rainfall Triggering of Landslides near Lisbon. Natural Hazards, 2005, 36, 331-354.	3.4	73
31	Rainfall patterns and critical values associated with landslides in Povoação County (São Miguel) Tj ETQq1 478-494.	1 0.784314 2.6	rgBT /Overlo 73
32	Comparison of model land skin temperature with remotely sensed estimates and assessment of surfaceâ€atmosphere coupling. Journal of Geophysical Research D: Atmospheres, 2015, 120, 12,096.	3.3	73
33	Chapter 3 Relations between variability in the Mediterranean region and mid-latitude variability. Developments in Earth and Environmental Sciences, 2006, , 179-226.	0.1	71
34	A deep learning approach for mapping and dating burned areas using temporal sequences of satellite images. ISPRS Journal of Photogrammetry and Remote Sensing, 2020, 160, 260-274.	11.1	63
35	Kalman filter physical retrieval of surface emissivity and temperature from geostationary infrared radiances. Atmospheric Measurement Techniques, 2013, 6, 3613-3634.	3.1	61
36	Explosive development of winter storm Xynthia over the subtropical North Atlantic Ocean. Natural Hazards and Earth System Sciences, 2013, 13, 2239-2251.	3.6	56

#	Article	IF	CITATIONS
37	An All-Weather Land Surface Temperature Product Based on MSG/SEVIRI Observations. Remote Sensing, 2019, 11, 3044.	4.0	55
38	Quality Assessment of S-NPP VIIRS Land Surface Temperature Product. Remote Sensing, 2015, 7, 12215-12241.	4.0	54
39	Cold Bias of ERA5 Summertime Daily Maximum Land Surface Temperature over Iberian Peninsula. Remote Sensing, 2019, 11, 2570.	4.0	49
40	Meteorological conditions associated with sea surges in Venice: a 40 year climatology. International Journal of Climatology, 2002, 22, 787-803.	3.5	47
41	Modelling directional effects on remotely sensed land surface temperature. Remote Sensing of Environment, 2017, 190, 56-69.	11.0	47
42	Kalman filter physical retrieval of surface emissivity and temperature from SEVIRI infrared channels: a validation and intercomparison study. Atmospheric Measurement Techniques, 2015, 8, 2981-2997.	3.1	47
43	Reference crop evapotranspiration derived from geo-stationary satellite imagery: a case study for the Fogera flood plain, NW-Ethiopia and the Jordan Valley, Jordan. Hydrology and Earth System Sciences, 2010, 14, 2219-2228.	4.9	44
44	The roles of NDVI and Land Surface Temperature when using the Vegetation Health Index over dry regions. Global and Planetary Change, 2020, 190, 103198.	3.5	44
45	Advancing land surface model development with satellite-based Earth observations. Hydrology and Earth System Sciences, 2017, 21, 2483-2495.	4.9	39
46	Incoming Solar and Infrared Radiation Derived from METEOSAT: Impact on the Modeled Land Water and Energy Budget over France. Journal of Hydrometeorology, 2012, 13, 504-520.	1.9	37
47	Satelliteâ€Based Assessment of Land Surface Energy Partitioning–Soil Moisture Relationships and Effects of Confounding Variables. Water Resources Research, 2019, 55, 10657-10677.	4.2	37
48	Calibration of the Fire Weather Index over Mediterranean Europe based on fire activity retrieved from MSG satellite imagery. International Journal of Wildland Fire, 2014, 23, 945.	2.4	35
49	How well do global burned area products represent fire patterns in the Brazilian Savannas biome? An accuracy assessment of the MCD64 collections. International Journal of Applied Earth Observation and Geoinformation, 2019, 78, 318-331.	2.8	35
50	Contribution of Land Surface Temperature (TCI) to Vegetation Health Index: A Comparative Study Using Clear Sky and All-Weather Climate Data Records. Remote Sensing, 2018, 10, 1324.	4.0	34
51	Correction of 2Âm-temperature forecasts using Kalman Filtering technique. Atmospheric Research, 2008, 87, 183-197.	4.1	33
52	A Thermodynamically Based Model for Actual Evapotranspiration of an Extensive Grass Field Close to FAO Reference, Suitable for Remote Sensing Application. Journal of Hydrometeorology, 2016, 17, 1373-1382.	1.9	33
53	Fire danger rating over Mediterranean Europe based on fire radiative power derived from Meteosat. Natural Hazards and Earth System Sciences, 2018, 18, 515-529.	3.6	33
54	Assessing the potential of parametric models to correct directional effects on local to global remotely sensed LST. Remote Sensing of Environment, 2018, 209, 410-422.	11.0	32

#	Article	IF	CITATIONS
55	Remote Sensing of Global Daily Evapotranspiration based on a Surface Energy Balance Method and Reanalysis Data. Journal of Geophysical Research D: Atmospheres, 2021, 126, e2020JD032873.	3.3	32
56	Validation of reference evapotranspiration from Meteosat Second Generation (MSG) observations. Agricultural and Forest Meteorology, 2018, 259, 271-285.	4.8	31
57	On precursors of South American cyclogenesis. Tellus, Series A: Dynamic Meteorology and Oceanography, 2007, 59, 114-121.	1.7	30
58	Moisture Sources and Large-Scale Dynamics Associated With a Flash Flood Event. Geophysical Monograph Series, 0, , 111-126.	0.1	30
59	Clear-Sky Window Channel Radiances: A Comparison between Observations and the ECMWF Model. Journal of Applied Meteorology and Climatology, 2003, 42, 1463-1479.	1.7	29
60	Quantifying the Clear‣ky Bias of Satellite Land Surface Temperature Using Microwaveâ€Based Estimates. Journal of Geophysical Research D: Atmospheres, 2019, 124, 844-857.	3.3	29
61	Landâ€Atmosphere Drivers of Landscape cale Plant Water Content Loss. Geophysical Research Letters, 2020, 47, e2020GL090331.	4.0	27
62	Estimation of downward longâ€wave radiation at the surface combining remotely sensed data and NWP data. Journal of Geophysical Research, 2010, 115, .	3.3	26
63	Large-Scale Atmospheric Circulation Driving Extreme Climate Events in the Mediterranean and its Related Impacts. , 2012, , 347-417.		25
64	Role of vegetation in representing land surface temperature in the CHTESSEL (CY45R1) and SURFEX-ISBA (v8.1) land surface models: a case study over Iberia. Geoscientific Model Development, 2020, 13, 3975-3993.	3.6	25
65	An innovative physical scheme to retrieve simultaneously surface temperature and emissivities using high spectral infrared observations from IASI. Journal of Geophysical Research, 2012, 117, .	3.3	22
66	Inversion of AMSR observations for land surface temperature estimation: 2. Global comparison with infrared satellite temperature. Journal of Geophysical Research D: Atmospheres, 2017, 122, 3348-3360.	3.3	22
67	Land Surface Albedo Derived on a Ten Daily Basis from Meteosat Second Generation Observations: The NRT and Climate Data Record Collections from the EUMETSAT LSA SAF. Remote Sensing, 2018, 10, 1262.	4.0	21
68	Daily grass reference evapotranspiration with Meteosat Second Generation shortwave radiation and reference ET products. Agricultural Water Management, 2021, 248, 106543.	5.6	19
69	A Methodology to Simulate LST Directional Effects Based on Parametric Models and Landscape Properties. Remote Sensing, 2018, 10, 1114.	4.0	18
70	Upgrading Land over and Vegetation Seasonality in the ECMWF Coupled System: Verification With FLUXNET Sites, METEOSAT Satellite Land Surface Temperatures, and ERA5 Atmospheric Reanalysis. Journal of Geophysical Research D: Atmospheres, 2021, 126, e2020JD034163.	3.3	17
71	Enhancing the fire weather index with atmospheric instability information. Environmental Research Letters, 2020, 15, 0940b7.	5.2	16
72	A New Method to Estimate Reference Crop Evapotranspiration from Geostationary Satellite Imagery: Practical Considerations. Water (Switzerland), 2019, 11, 382.	2.7	15

#	Article	IF	CITATIONS
73	Validation and consistency assessment of land surface temperature from geostationary and polar orbit platforms: SEVIRI/MSG and AVHRR/Metop. ISPRS Journal of Photogrammetry and Remote Sensing, 2021, 175, 282-297.	11.1	15
74	A multi-sensor approach to retrieve emissivity angular dependence over desert regions. Remote Sensing of Environment, 2020, 237, 111559.	11.0	14
75	A Practical Method for High-Resolution Burned Area Monitoring Using Sentinel-2 and VIIRS. Remote Sensing, 2021, 13, 1608.	4.0	14
76	Intercalibration of NOAA and Meteosat window channel brightness temperatures. International Journal of Remote Sensing, 2005, 26, 3717-3733.	2.9	13
77	A Physically Constrained Calibration Database for Land Surface Temperature Using Infrared Retrieval Algorithms. Remote Sensing, 2016, 8, 808.	4.0	13
78	The summer diurnal cycle of coastal cloudiness over west Iberia using Meteosat/SEVIRI and a WRF regional climate model simulation. International Journal of Climatology, 2016, 36, 1755-1772.	3.5	13
79	A New Retrieval Algorithm for Soil Moisture Index from Thermal Infrared Sensor On-Board Geostationary Satellites over Europe and Africa and Its Validation. Remote Sensing, 2019, 11, 1968.	4.0	12
80	Synergistic use of the two-temperature and split-window methods for land-surface temperature retrieval. International Journal of Remote Sensing, 2010, 31, 4387-4409.	2.9	10
81	Quality assessment and improvement of the EUMETSAT Meteosat Surface Albedo Climate Data Record. Atmospheric Measurement Techniques, 2015, 8, 4561-4571.	3.1	10
82	Surface Albedo Retrieval from 40-Years of Earth Observations through the EUMETSAT/LSA SAF and EU/C3S Programmes: The Versatile Algorithm of PYALUS. Remote Sensing, 2021, 13, 372.	4.0	10
83	Improving Land Surface Temperature Retrievals over Mountainous Regions. Remote Sensing, 2017, 9, 38.	4.0	9
84	Evaluation of Two Global Land Surface Albedo Datasets Distributed by the Copernicus Climate Change Service and the EUMETSAT LSA-SAF. Remote Sensing, 2020, 12, 1888.	4.0	9
85	Observed Landscape Responsiveness to Climate Forcing. Water Resources Research, 2022, 58, .	4.2	9
86	Modelling of Wine Production Using Land Surface Temperature and FAPAR—The Case of the Douro Wine Region. Remote Sensing, 2019, 11, 604.	4.0	8
87	Satellite Retrieval of Downwelling Shortwave Surface Flux and Diffuse Fraction under All Sky Conditions in the Framework of the LSA SAF Program (Part 2: Evaluation). Remote Sensing, 2019, 11, 2630.	4.0	8
88	Satellite Retrieval of Downwelling Shortwave Surface Flux and Diffuse Fraction under All Sky Conditions in the Framework of the LSA SAF Program (Part 1: Methodology). Remote Sensing, 2019, 11, 2532.	4.0	8
89	Integrating Reanalysis and Satellite Cloud Information to Estimate Surface Downward Long-Wave Radiation. Remote Sensing, 2022, 14, 1704.	4.0	8
90	Downscaling Meteosat Land Surface Temperature over a Heterogeneous Landscape Using a Data Assimilation Approach. Remote Sensing, 2016, 8, 586.	4.0	7

#	Article	IF	CITATIONS
91	Multisensor Thermal Infrared and Microwave Land Surface Temperature Algorithm Intercomparison. Remote Sensing, 2020, 12, 4164.	4.0	4
92	A Comprehensive Clear-Sky Database for the Development of Land Surface Temperature Algorithms. Remote Sensing, 2022, 14, 2329.	4.0	1
93	Land surface albedo and downwelling shortwave radiation from MSG geostationary satellite: Method for retrieval, validation, and application. , 2011, , .		0